PHYSICAL REVIEW B VOLUME 44, NUMBER 22 1 DECEMBER 1991-II

Spin polarization and magnetic dichroism in photoemission from core and valence states in localized magnetic systems

B. T. Thole
Materials Science Centre, University of Groningen, Nijenborgh 16, 9747 AG Groningen, The Netherlands

G. van der Laan
SERC Daresbury Laboratory, Warrington WA4 4AD, United Kingdom

(Received 10 April 1991)

Using group theory we derive a general model for spin polarization and magnetic dichroism in photoemission in the presence of atomic interactions between the hole created and the valence holes. We predict strong effects in the photoemission from core levels and localized valence levels of transition metal and rare-earth compounds. In the presence of electrostatic interactions between the created hole and magnetically polarized valence electrons, we can distinguish eight fundamental spectra: the isotropic spectrum, spin spectrum, orbit spectrum (magnetic circular dichroism), spin-orbit spectrum, spin-orbit magnetic-quadrupole spectrum, anisotropic spectrum (magnetic linear dichroism), anisotropic spin magnetic-dipole spectrum , and anisotropic spin magnetic-octupole spectrum. Examples are given for the 2*p*, 3*s*, 3*p*, and 3*d* photoemission from divalent Cu, Co d^7, and Fe d^6.

I. INTRODUCTION

There is a widespread belief among solid-state physicists that the spin polarization in core-level photoemission is uniquely determined by optical-spin orientation, the so-called Fano effect.[1] This is because the atomiclike core level and free-electron-like photoelectron state are not directly influenced by a polarized valence shell, leaving the core-hole–spin-orbit coupling as the remaining interaction. Until recently,[2] it was also believed that core-level photoemission hardly depends on the linear or circular polarization of the incident photon, except in the near-threshold region. However, these impressions are wrong when there are electrostatic interactions between the spin and orbital momenta of the valence state and core hole. In transition-metal, rare-earth, and actinide compounds, the core hole interacts strongly with the valence *d* (or *f*) electrons, which may result both in a strong spin polarization and in a magnetic dichroism in photoemission.

It is well known that core-hole spectroscopy can be used to determine essential properties of the electronic structure of the valence band in localized materials.[3,4] In 3*d* and 4*f* materials the appearance of multiplet and satellite structure indicates the presence of electrostatic interactions and hybridization. It is the purpose of this article to show that these structures can be further separated into spin and orbit information using spin-polarized detection. So far only a few experiments have been performed on core levels. Since spin-polarization measurements require the use of synchrotron radiation as a powerful and tunable source, they are most easily done in the vacuum ultraviolet region (<40 eV), which covers the valence bands, but not the deeper core levels. However, the recent progress in synchrotron-radiation instrumentation has also made the soft-x-ray region accessible. Plane-polarized radiation can be obtained by using the paraxial radiation from the synchrotron-radiation source, and a high degree of circularly polarized radiation can be obtained by a helical or crossed undulator,[5] a quarter-wave plate, a Goedkoop filter,[6] or most commonly, an inclined-angle view of the tangent point of the stored electron beam.

Although a connection between x rays and magnetic structure had already been searched for much earlier,[7] experimental observation was made only in 1986 in magnetic x-ray dichroism.[8] This discovery was followed by research in related phenomena where the cross section for x-ray scattering depends on the polarization of the x rays, such as magnetic resonant scattering,[9–12] magnetic Kerr effect,[13] and Faraday rotation.[14] Also, polarization effects were found in core-hole photoemission. Hillebrecht, Jungblut, and Kisker[15] and Carbone *et al.*[16–18] observed spin polarization in Fe 3*s* and 3*p* core-level photoemission and Baumgarten *et al.*[2] observed magnetic circular dichroism in the Fe 2*p* core-level photoemission of ferromagnetic iron.[19,20] We may expect a rapid further development in core-level photoemission using polarized x rays and spin detection.

Because of its close relation to core-hole emission, this paper would not be complete without a summarization of the rapid development which has been made in the last two decades in the field of spin-polarized *valence-band* photoemission from solids with spin orbit and exchange-split bands.[21–23] Research in this area has produced a wealth of information on the electronic and magnetic properties of ferromagnetic metals, alloys, thin films, and adsorbates and has had an important impact on the development of modern theories of magnetism, such as, e.g., in the field of surface magnetism. The calculations by Fano[1] on the spin orientation of photoelectrons from Cs vapor, produced by circularly polarized light and the detection of spin-polarized photoemission from ferromagnets,[24] have contributed largely to this development. The spin polarization in valence-band photoemission from solids has been explained with band-structure calculations, where each electron moves independently in a relativistic potential, which takes into account spin-dependent exchange and spin-orbit interaction.[21] In ferromagnetic $3d$ transition metals the valence band is oriented by exchange interaction, and since the photoelectrons retain their spin orientation during the excitation process, spin-polarized photoemission reflects the majority- and minority-spin density of states. In $4d$ and $5d$ transition metals the valence band is split by spin-orbit interaction, and a polarized optical excitation gives polarization of the orbital momentum which is coupled to the spin. This phenomenon, which is sometimes called optical spin orientation or Fano effect, allows one to do a symmetry-resolved band mapping of the valence bands. Even with linearly polarized or isotropic radiation, excitation from level which has spin-orbit interaction can be spin polarized in the angular-dependent emission due to interference between the two different final-state wave functions with $\Delta l = \pm 1$.[25,26] Thus spin polarization of the total photoemission in the one-electron model requires either spin-orbit coupling or exchange splitting of the valence levels, because the electric vector does not act directly on the electron spin.

A related effect in valence-band photoemission, but where the spin polarization is not measured, is magnetic circular dichroism. Here the polarization of the electric light vector and spin orientation in magnetic materials are coupled by the spin-orbit interaction. In nonmagnetic materials with negligible spin-orbit interaction, the angle-integrated photoemission is independent of the light polarization, but in a chiral sample or chiral geometry, there can be circular dichroism in the angular distribution (CDAD) of photoelectrons.[27–29] The distribution depends on the radial dipole matrix elements and phase difference between the final-state wave functions.

In this paper we give a general formulation of spin polarization and magnetic dichroism from localized states and core levels which have electrostatic interactions. These effects can be analyzed using angular momentum coupling.[30] In order to exclude additional effects, we take into account only one final-state channel and a constant radial matrix element for electron excitation from the core level to the continuum, which has zero spin-orbit and electrostatic interactions. For photoemission far above the continuum onset, the $\Delta l = +1$ channel dominates and the error in these approximations will be small. We do take into account the hybridization in the ground and final state, although in the group theory only spherical hybridization will be treated.

The paper is organized as follows. First, we derive group-theoretical results for spin-resolved photoemission from a core level and from the valence band. A comparison is made with x-ray absorption. In Sec. III the results are explained in physical terms. We show that there are eight fundamental spectra, each describing a specific coupling between photon, photoelectron, and magnetic moment. Finally, using calculated spin-polarized photoemission spectra of $3d$ transition metals, we discuss the main features of the s core hole, the deep and shallow p core hole, and the d-valence-shell photoemission, which all have strongly different features.

II. THEORY

A. General theory of spin-polarized dipole transition spectra

Consider photoemission from a core level in an atom with an open shell, say, a transition-metal ion. We construct a complete basis $\langle \varphi_i |$ for the open-shell electrons. This basis may contain states from more than one configuration, thus taking into account hybridization. Without loss of generality we assume that φ_0 is the ground state. In order to avoid explicit use of fractional parentage coefficients, we add a shell with one hole to the ground state, with angular momentum l and spin momentum σ. This represents the l_ε continuum state to which the core electron is excited. In the final state this shell is filled and there is a hole in a core level with angular momentum p. The result is the same as when we use an empty l shell in the initial state or any other incompletely filled l shell. We denote the Z component of orbital and spin momentum by m and σ, respectively. Thus the ground state is

$$\langle g | = \langle \varphi_0 ; l m \sigma | \ , \tag{1}$$

and the final state is

$$| f \rangle = \sum_{i,k} C_{ik} | \varphi_i ; \underline{p} m_k \sigma_k \rangle \ , \tag{2}$$

where $\underline{p}$ denotes a core hole. The dipole matrix element between these states is, considering only transitions from core p to continuum l_ε,

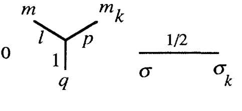

$$T_{mq\sigma} = \langle g | T_q^1 | f \rangle = \sum_{i,k} C_{ik} \langle \varphi_0 ; l m \sigma | T_q^1 | \varphi_i ; \underline{p} m_k \sigma_k \rangle = \sum_{i,k} C_{ik} \delta_{i0} \begin{array}{c} m \qquad m_k \\ {}^{l}\diagdown\!\diagup{}^{p} \\ {}_{1}| \\ q \end{array} \quad \underset{\sigma \qquad\qquad \sigma_k}{\overset{1/2}{\overline{\qquad\qquad}}} \ \langle l \| r \| p \rangle \ , \tag{3}$$

where T_q^1 is the dipole transition operator and where we have used the graphical representation of the 3-j and 2-j symbols.[30,31] In the following we will suppress the radial integral $\langle l \| r \| p \rangle$. The spin-polarized transition probability is

$$I_{q\sigma}=\sum_{m}|T_{mq\sigma}|^2=\sum_{k,k'}C_{0k}C_{0k'}$$

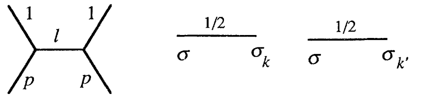

$$=\sum_{x}\sum_{k,k'}C_{0k}C_{0k'}$$

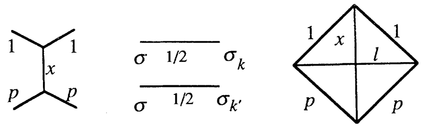

, (4)

where we have used theorem 2 of Yutsis, Levinson, and Vanagas (YLV2).[30,31] The graph with four free lines and the square represent a 4-j and 6-j symbol, respectively. From Eq. (4) we can derive the essential symmetry aspects of the analysis of the spectra. In many cases the coefficients C_{0k} have a special form, e.g., when φ_i and $\underline{p}$ are coupled by Coulomb interaction in a spherical system. Moreover, in high symmetry the ground state and excited states are degenerate, and we have to sum over the transition probabilities involved. As will be shown in four important examples, in such cases the summations together produce a recoupling coefficient which we will denote abstractly by a rectangular box in order to inspect the general properties of spin-polarized dipole spectra of ordered systems. In the derivations we will use the graphical techniques of Yutsis, Levinson,and Vanagas.[30,31] In order to suppress group-theoretical detail in favor of physical clarity, we omitted arrows in the graphs. In the few cases that matter we have added the correct signs into the equations. Further we suppressed dimensional factors. When there is a summation over a momentum, e.g., x, y, z, L, S, or J, we implicitly assume the summant to be multiplied by $2x+1$, $2y+1$, etc.

$$I_{q\sigma}=$$

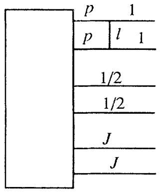

$$=\sum_{x,y,z}$$

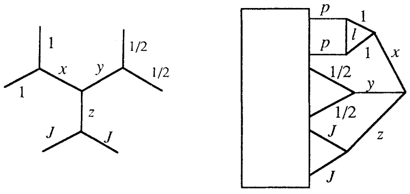

$$=\sum_{x,y,z}$$

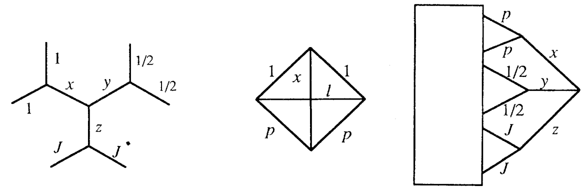

$$\equiv\sum_{x,y,z}P^{xyz}_{1(1/2)J}\,Q^{x}_{p1l}\,R^{xyz}_{p(1/2)J}\ . \tag{5}$$

Here J is added to the box to show explicitly the magnetic moment created in the ground state. It is the total angular momentum when there is spin-orbit coupling and it denotes S in the absence of spin-orbit coupling in the ground state. Such a total J or S is implicitly assumed in φ_0. We do not consider the case of an exchange or crystal field strong enough to mix different J or S values. We feel that important parts of our analysis remain valid in this case because most of the group theory can also be applied to point groups. But the subtle changes which are needed have to be analyzed in the future. Further, we assume that exchange field splitting in the final state is not resolvable experimentally and that we can sum the intensities over the degenerate final states involved. If these splittings could be resolved, the diagrams in Eq. (5) would have two additional free lines for the final state J or S, and then much more information could be extracted by an analysis analogous to the one presented here. The same applies to the measurement of the orbital angular momentum, but here we will assume that angle-integrated emission is measured.

Equation (5) reformulates the separation of $I_{q\sigma}$ as a sum of terms where three physical effects are separated. The factor P contains all the free lines and thus describes all polarization dependence of the spectra. Q contains all l dependence. This means that if we know the spectra for transitions to one value of l_ε, we can obtain the spectra for the other l_ε value in a trivial way, discussed in Sec.

III. The factor R contains the information on the coupling of the magnetic moment, photon, and photoelectron spin depending on the final state considered.

We can now define the six *fundamental* spectra I^{xy}. These are meant to be linear combinations of the *primitive* spectra $I_{q\sigma}$ that are especially powerful because they extract the essential data and each fundamental spectrum measures its own physical effect:

$$I^{xy} \equiv \sum_{q,\sigma} (-1)^{1-q} \begin{bmatrix} 1 & x & 1 \\ -q & 0 & q \end{bmatrix} (-1)^{1/2-\sigma} \begin{bmatrix} \frac{1}{2} & y & \frac{1}{2} \\ -\sigma & 0 & \sigma \end{bmatrix} I_{q\sigma}$$

$$= \sum_{q,\sigma}$$

$$I_{q\sigma}$$

$$= \sum_{x',y',z}$$

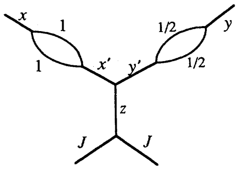

$$Q^{x}_{p1l} R^{xyz}_{p(1/2)J} = \sum_{z}$$

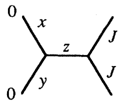

$$Q^{x}_{p1l} R^{xyz}_{p(1/2)J}$$

$$= \sum_{z}$$

$$Q^{x}_{p1l} R^{xyz}_{p(1/2)J} \,. \qquad (6)$$

Because of the triads $\{1\,x\,1\}$ and $\{\frac{1}{2}\,y\,\frac{1}{2}\}$, the values of x can be 0, 1, and 2 and y can be 0 and 1. Thus there are six independent spectra. The use of 3-j symbols in the definition of I^{xy} is for reasons of elegance. For the interpretation of the spectra, constant factors are of little importance. The essential property is their proportionality to q and $3q^2-2$:

$$\begin{aligned} (-1)^{1-q} \begin{bmatrix} 1 & x & 1 \\ -q & 0 & q \end{bmatrix} &= \frac{1}{\sqrt{3}} \quad (x=0) \\ &= \frac{q}{\sqrt{6}} \quad (x=1) \\ &= \frac{3q^2-2}{\sqrt{30}} \quad (x=2)\,, \end{aligned} \qquad (7)$$

$$\begin{aligned} (-1)^{1/2-\sigma} \begin{bmatrix} \frac{1}{2} & y & \frac{1}{2} \\ -\sigma & 0 & \sigma \end{bmatrix} &= \tfrac{1}{2} \quad (y=0) \\ &= \frac{\sigma}{\sqrt{3/2}} \quad (y=1)\,. \end{aligned} \qquad (8)$$

We write out explicitly all $I^{xy} = \sum_z I^{xyz}$, where the eight fundamental spectral I^{xyz} will be defined in Eq. (17) and $\sigma = -\frac{1}{2}, \frac{1}{2}$ is denoted by $\downarrow, \uparrow$:

$$I^{00} = I^{000} = (I_{1\uparrow} + I_{0\uparrow} + I_{-1\uparrow} + I_{1\downarrow} + I_{0\downarrow} + I_{-1\downarrow})/(2\sqrt{3})\,, \qquad (9)$$

$$I^{01} = I^{011} = (I_{1\uparrow} + I_{0\uparrow} + I_{-1\uparrow} - I_{1\downarrow} - I_{0\downarrow} - I_{-1\downarrow})/(3\sqrt{2}), \qquad (10)$$

$$I^{10} = I^{101} = (I_{1\uparrow} - I_{-1\uparrow} + I_{1\downarrow} - I_{-1\downarrow})/(2\sqrt{6})\,, \qquad (11)$$

$$I^{11} = I^{110} + I^{112} = (I_{1\uparrow} - I_{-1\uparrow} - I_{1\downarrow} + I_{-1\downarrow})/3\,, \qquad (12)$$

$$I^{20} = I^{202} = (I_{1\uparrow} - 2I_{0\uparrow} + I_{-1\uparrow} + I_{1\downarrow} - 2I_{0\downarrow} + I_{-1\downarrow})/(2\sqrt{30})\,, \qquad (13)$$

$$I^{21} = I^{211} + I^{213} = (I_{1\uparrow} - 2I_{0\uparrow} + I_{-1\uparrow} - I_{1\downarrow} + 2I_{0\downarrow} - I_{-1\downarrow})/(3\sqrt{5})\,. \qquad (14)$$

The sum over z is from $|x-y|$ to $(x+y)$, but $x+y+z$ must be even because

$$\begin{bmatrix} x & y & z \\ 0 & 0 & 0 \end{bmatrix} = 0 \quad (x+y+z=\text{odd}) . \tag{15}$$

I^{xy} contains one z value when x or y is 0; else it contains the sum over two values of z, i.e., $z=x-1$, $x+1$, because $z=x$ is forbidden.

Inspection of the linear combinations for I^{xy} shows that we need all six $I_{q\sigma}$ to obtain all I^{xy}. But each individual I^{xy} can be obtained in a simpler way. The spectra with $x=0$ can be obtained with isotropic light or an isotropic sample; $x=1$ only needs the difference spectrum of left and right circularly polarized light and $x=2$ measures the difference between Z- and XY-linearly polarized light or between Z- and isotropically polarized light. Likewise, $y=0$ does not need spin-polarization measurement, and $y=1$ measures the difference between up and down spin. Finally, instead of reversing the polarization of the light or spin polarization, we can also reverse the magnetization because, in an obvious notation, $I_{q\sigma M} = I_{-q-\sigma-M}$.

The intensity I^{xy} in Eq. (6) contains the factor

$$F^z_{JM} \equiv$$

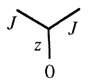

$$= (-1)^{J-M} \begin{bmatrix} J & z & J \\ -M & 0 & M \end{bmatrix} . \tag{16}$$

This factor is proportional to the Z component of the zth moment of the ground-state magnetic moment. For $z=0$ the factor is $|J|^{-1/2}$, independent of M: therefore, a $z=0$ term does not depend on the polarization of the ground state. For $z=1$ the factor is $M/[J(J+1)(2J+1)]^{1/2}$, proportional to M. Such a term is proportional to the magnetic moment of the ion.

In the same way F^2_{JM} is proportional $3M^2-J(J+1)$, the Z component of the electric and magnetic quadrupole. It can be interpreted as the deviation from sphericity because it is $\langle 3J_z^2 - J^2 \rangle$. This term can be present when $\langle F^1_{JM} \rangle = 0$, as in antiferromagnets, or when the ion is polarized by a crystal field, which keeps M and $-M$ degenerate. It is required that $J \geq 1$. F^3_{JM} measures a still higher moment of the atom: $5M^3 - 3MJ(J+1)$.

When we need a distribution over different M values, because of temperature effects or in antiferro- or ferrimagnets, we can treat this effect by taking the expectation value of the 3-j symbol, because it contains all M dependence. Whenever needed, we can read $\langle F^z_{JM} \rangle$ instead of F^z_{JM}.

The possible values of z for each I^{xy} show what ground-state polarization is needed to obtain a nonzero spectrum: I^{00} needs no polarization. I^{10} and I^{01} need $z=1$, i.e., a magnetic moment. I^{20} needs $z=2$, i.e., a quadrupole moment. I^{11} needs no polarization ($z=0$), but a quadrupole moment ($z=2$) gives an extra contribution. I^{21} needs $z=1$ or $z=3$ (octupole).

Our situation would clearly be perfect if we would be able to measure

$$I^{xyz} = I_{q\sigma M} F^x_{1q} F^y_{(1/2)\sigma} F^z_{JM} , \tag{17}$$

in which case all eight spectra I^{xyz} could be separated, but it clearly requires $I_{q\sigma M}$ to be measured for all M, which we consider impractical because we would have to populate those M levels specifically. Therefore, we chose I^{xy} with the small disadvantage that in two spectra z is summed over two terms.

It is clear that the linear combinations I^{xy} separate different ground-state effects in a meaningful way. But inspection of the symmetry and physics of the interactions that couple the ground-state moment, the photon spin and the photoelectron spin give even more meaning. For reasons of space a full derivation will only be shown in two cases. In the other cases only the result is shown. The derivations take into account spherical hybridization because no use is made of any single-configuration formalism.

Sections II B and II C treat shallow and deep core-hole level x-ray photoelectron spectroscopy (XPS) of transition-metal compounds without spin-orbit coupling in the ground state. Sections II D and II E apply to shallow and deep core-level XPS of transition metals and heavier atoms with spin-orbit coupling in the ground state. Section II E discusses various cases of valence-band XPS.

B. Ground-state $LS \rightarrow$ final-state LS

The simplest case is obtained when there is no core or valence spin-orbit interaction. We will take, for the ground state,

$$\langle g | = \langle LS; lm\sigma | \tag{18}$$

and, for the final state,

$$| f \rangle = \sum_{L'S'} C_{L'S'\underline{L}\underline{S}} | (L'S'p\tfrac{1}{2})\underline{L}\underline{S} \rangle , \tag{19}$$

where the $L'S'$ are the complete set of valence-shell states. They are coupled with the core hole $p\frac{1}{2}$ to a total $\underline{L}\underline{S}$ state. Because of the triangular relations, L' can only be $\underline{L}-1$, $\underline{L}$, or $\underline{L}+1$, and S' can be $\underline{S}-\frac{1}{2}$ and $\underline{S}+\frac{1}{2}$.

The dipole matrix element is (omitting the radial matrix element)

$$\langle g | T_q | f \rangle = C_{LS\underline{L}\underline{S}}$$

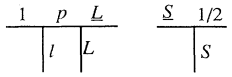

$$. \tag{20}$$

For the total intensity we have to sum the square of the matrix element over m, M_L, $M_{\underline{S}}$, and $M_{\underline{L}}$, where the M denote Z components of the quantum numbers in the subscript. The sum over m is needed because we measure all photoelectrons, irrespective of their m value. We sum M_L because in the ground state the spin S is split by the exchange field, but the sublevels of L remain degenerate. Finally, $M_{\underline{L}}$ and $M_{\underline{S}}$ label the degenerate final-state sublevels of $\underline{L}$ and $\underline{S}$:

$$I_{q\sigma}=C^2_{LS\underline{LS}}$$

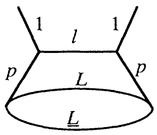

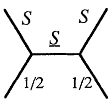

$$=C^2_{LS\underline{LS}}$$

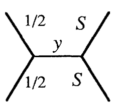

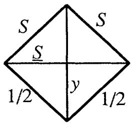

. (21)

The photon spin has disappeared, and therefore we have no value for x in this case. The spectrum is independent of the polarization of the photon. Without spin-orbit coupling, the photon, which acts only on the orbit, is not sensitive to the ground-state spin and cannot polarize the photoelectron spin. The latter spin is polarized directly by Coulomb interaction with the polarized ground state:

$$I^y=C^2_{LS\underline{LS}}$$

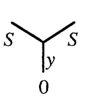

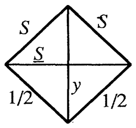

$$=C^2_{LS\underline{LS}}\langle S_z^{(y)}\rangle_g\langle(S\tfrac{1}{2})\underline{S}\|(yy)0\|(S\tfrac{1}{2})\underline{S}\rangle$$

$$=C^2_{LS\underline{LS}}\langle S_z^{(y)}\rangle_g\langle S_d^{(y)}\cdot s_p^{(y)}\rangle_f\ . \quad (22)$$

The last two steps have no completely defined meaning. They only reexpress the 3-j and 6-j symbols in a matrix-element-type fashion, to show that I^y is determined by expectation values of operators with a specific symmetry.

The isotropic spectrum can be denoted by $I^0=I_\uparrow+I_\downarrow$ without specification of q:

$$I^0=C^2_{LS\underline{LS}}\ , \quad (23)$$

$$I^1=C^2_{LS\underline{LS}}\langle S_z\rangle_g\langle S_d\cdot s_p\rangle_f\ . \quad (24)$$

We see that I^1 is proportional to the ground-state magnetic moment $\langle S_z\rangle$. The final-state-type matrix element has the symmetry of a spin-spin coupling operator. It measures the inner product of the d-shell spin S and the core-hole spin s. Thus, when the ground state S is polarized and a transition is made to a state where S and s are aligned, then s is also polarized, and because s is equal to the spin of the photoelectron, we measure a difference between ↑ and ↓ spin, which is I^1. Note that the final-state-type matrix element is not really an expectation value in the excited state, because $C_{L'S'\underline{LS}}|(L'S'p\tfrac{1}{2})\underline{LS}\rangle$ is only a part of the final-state wave function. Therefore, XPS measures only a part of the final-state wave function and the I^1 intensity is given by the correlation of core and valence spin in that part.

The 6-j symbol in I^1 is simple and interesting enough to be written out explicitly:

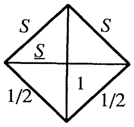

$$=\frac{\underline{S}(\underline{S}+1)-S(S+1)-\frac{3}{4}}{[6S(S+1)(2S+1)]^{1/2}}$$

$$\propto\begin{cases}S & (\underline{S}=S+\frac{1}{2})\\ -S-1 & (\underline{S}=S-\frac{1}{2})\end{cases}\ . \quad (25)$$

So we see that high-spin final states ($\underline{S}=S+\frac{1}{2}$) give a positive peak ($S$) and low-spin states give a negative peak ($-S-1$). Also the low-spin peak is stronger by a factor $(S+1)/S$.

There are two useful and equivalent ways of interpreting the I^1 spectrum. For the first we look at Eq. (25) and see that high- and low-spin final states give different peaks. For the second we look at Eq. (22) and see that when S_d and s_p are parallel (antiparallel) we have a positive (negative) peak. The equivalence lies in the fact that in the high- (low-) spin state the spins are parallel (antiparallel). This duality of interpretation also arises in other cases.

C. Ground-state $LS\rightarrow$ final-state J

In order to get dependence of the photoelectron spin on the photon spin, there has to be spin-orbit coupling. First, we treat the case that there is spin-orbit coupling in the final state (in the core hole). For this we couple $\underline{L}$ and $\underline{S}$ to a total $\underline{J}$ and sum over $\underline{L}$ and $\underline{S}$:

$$\langle g|=\langle LS;lm\sigma|\ , \quad (26)$$

$$|f\rangle=\sum_{L,S,\underline{L},\underline{S}}C_{LS\underline{LS}}|(LSp\tfrac{1}{2})\underline{LSJ}\rangle=\sum_{L,S,\underline{L},\underline{S}}C_{LS\underline{LS}}|(LSp\tfrac{1}{2})\underline{LS}\rangle$$

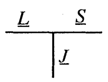

, (27)

$$\langle g|T_q|f\rangle=\sum_{\underline{LS}}C_{LS\underline{LS}}$$

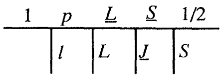

, (28)

$$I_{q\sigma}=\sum_{M_l,M_L,M_{\underline{J}}}|\langle g|T_q|f\rangle|^2=\sum_{\underline{L},\underline{S},\underline{L}_1,\underline{S}_1}C_{LS\underline{LS}}C_{LS\underline{L}_1\underline{S}_1}$$

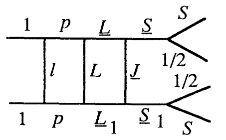

, (29)

$$I^{xy}=\sum_{z,\underline{L},\underline{S},\underline{L}_1,\underline{S}_1} C_{LS\underline{LS}}C_{LS\underline{L}_1\underline{S}_1}$$

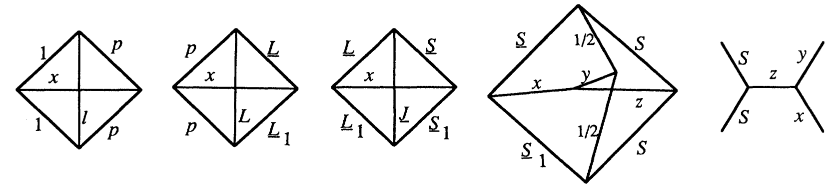

, (30)

$$R^{xyz}_{p(1/2)S}=\sum_{\underline{L},\underline{S},\underline{L}_1,\underline{S}_1} C_{LS\underline{LS}}C_{LS\underline{L}_1\underline{S}_1}\langle (LSp\tfrac{1}{2})\underline{LSJ}\|(0zxy)xx0\|(LSp\tfrac{1}{2})\underline{L}_1\underline{S}_1\underline{J}\rangle$$

$$=\sum_{\underline{L},\underline{S},\underline{L}_1,\underline{S}_1} C_{LS\underline{LS}}C_{LS\underline{L}_1\underline{S}_1}\langle [[S_d^{(z)}s_p^{(y)}]^{(x)}l_p^{(x)}]^{(0)}\rangle_f \equiv \langle S_d^{(z)}\cdot s_p^{(y)}\cdot l_p^{(x)}\rangle_f \;. \tag{31}$$

This shows what kind of correlation is needed to observe a term z in I^{xy}. The definition of the "triple scalar product" in Eq. (31) is given to express that the correlation is symmetrical in the three moments. The xth moment of the core orbit, the yth moment of the core spin, and the zth moment of the valence spin must be correlated. The names of the operators are only to indicate at what orbital or spin they operate. Thus $S_d^{(z)}$ is an operator of symmetry z acting on the spin of the d shell. The actual values of the matrix elements are given by Eq. (30). S_d, s_p, and l_p may be seen as unit operators. We are not interested in their magnitude, but only in the amount of correlation between their components.

The operator in Eq. (31) looks complicated, but when one or two of the moments x,y,z are zero, the interpretation is easy. I^{000} does not measure any coupling between S_d, s_p, and l_p.

I^{101} measures $\langle S_d\cdot l_p\rangle$, which is the alignment of the induced moment with the core orbit. For such a correlation we need p-d interactions, i.e., p-d Coulomb and exchange interactions plus spin-orbit interaction in valence or core shell to correlate spin and orbit. We see that the group theory only tells us what moments must be correlated. The physics of the problem tells us how this is achieved. Section III discusses the possible ways of coupling in detail. We will give here a short explanation of the other spectra.

I^{011} measures $\langle S_d\cdot s_p\rangle$, the alignment of the core-hole spin with the induced valence moment. It is positive (negative) in high- (low-) spin final states. In the final state the total spin is not a good quantum number, but we can say that I^{101} measures the spin *character*.

When we designate a peak as positive or negative, this refers to the channel $l_\varepsilon=l_p-1$. In the channel $l_\varepsilon=l_p+1$, the spectra with odd x are reversed (cf. Sec. III).

I^{110} measures $\langle s_p\cdot l_p\rangle$, i.e., the core-hole spin-orbit energy. It is positive for $2p_{3/2}$, where l_p and s_p are parallel, negative in $2p_{1/2}$.

I^{202} measures $\langle l_p^{(2)}\cdot S_d^{(2)}\rangle$, the correlation between the anisotropies of core orbit and induced moment. These higher-moment correlations are difficult to interpret, but we can still determine what interactions are needed to cause such correlations.

I^{211}, I^{213}, and I^{112} require S_d, l_p, and s_p to be all correlated with each other. However, it is generally sufficient that, e.g., S_d is aligned with s_p, by Coulomb interactions, and that s_p is aligned with l_p, by core spin-orbit interactions, to have S_d be aligned with l_p. In the following coupling cases we will see two other slightly different ways to couple the three momenta.

D. Ground-state $LSJ\rightarrow$ final-state LS

Spin-orbit coupling in the valence band couples L and S immediately to the induced polarization of J:

$$\langle g|=\langle LSJ;lm\sigma|=\langle LS;lm\sigma|$$

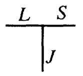

, (32)

$$|f\rangle=\sum_{L',S'} C_{L'S'\underline{LS}}|(L'S'p\tfrac{1}{2})\underline{LS}\rangle \;, \tag{33}$$

$$\langle g|T_q|f\rangle=C_{LS\underline{LS}}$$

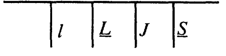

, (34)

$$I_{q\sigma}=\sum_{M_l,M_{\underline{L}},M_{\underline{S}}} |\langle g|T_q|f\rangle|^2 \;, \tag{35}$$

$$R^{xyz}_{p(1/2)J}=C^2_{LS\underline{LS}}\langle [L_d^{(x)}S_d^{(y)}]^{(z)}\rangle_g \times\langle [L_d^{(x)}\cdot l_p^{(x)}][S_d^{(y)}\cdot s_p^{(y)}]\rangle_f \;. \tag{36}$$

The interpretation here is that $L_d^{(x)}$ and $S_d^{(y)}$ are coupled to a total moment z.

Now, when $l_p^{(x)}$ is coupled to $L_d^{(x)}$ and $s_p^{(y)}$ to $S_d^{(y)}$, they are automatically coupled to the induced moment. The coupling in the ground state is determined by spin-orbit coupling. Thus, for $x=0$, $y=1$, the ground-state expectation value in Eq. (36) measures $\langle S_d\rangle$. Multiplied by the factor F^z_{JM}, the intensity I^{01} thus measures $\langle S_Z\rangle_g$, the component of the spin parallel to the total moment. This is always negative because the exchange field acts on S (and μ_B is negative), but for less than half-filled shells

$\langle L_Z \rangle_g$ is positive in the Hund's rule ground state because the spin-orbit coupling directs L antiparallel to S. For the same reason $\langle L_d \cdot S_d \rangle$ is negative. For more than half-filled shells $\langle L_Z \rangle_g$ is negative and $\langle L_d \cdot S_d \rangle$ is positive. The values of these and higher-moment ground-state correlations are given by angular algebra (9-j symbol) when L and S are good quantum numbers.

It is interesting to note that, for $x=0$, Eq. (36) is the same as Eq. (22). Thus, without spin-orbit coupling in the final state, the isotropic spectrum and spin spectrum are not sensitive to (a small) spin-orbit coupling in the ground state. The other spectra $x \neq 0$ do need spin-orbit coupling in the ground or final state.

E. Ground-state $LSJ \rightarrow$ final-state J

Here we analyze the case where there is both valence band and core-hole spin-orbit interaction. The ground state is the same as in Eq. (32), and the final state is taken from the $LS \rightarrow J$ case:

$$\langle g| = \langle LSJ; lm\sigma| = \langle LS; lm\sigma| \qquad (37)$$

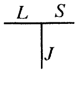

$$|f\rangle = \sum_{L',S',J',j} C_{L'S'J'jJ} |L'S'J'p\tfrac{1}{2}j\underline{J}\rangle$$

$$= \sum_{\underline{L},\underline{S},L',S',J',j} C_{L'S'J'j\underline{J}} |L'S'p\tfrac{1}{2}\underline{LS}\rangle \qquad (38)$$

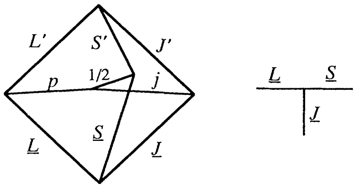

$$\langle g|T_q|f\rangle = \sum_{\underline{L},\underline{S},j} C_{LSJj\underline{J}}$$

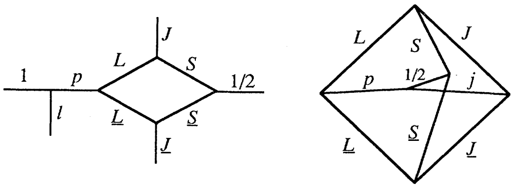

$$= \sum_j C_{LSJj\underline{J}} \qquad (39)$$

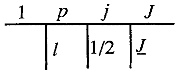

$$I_{q\sigma} = \sum_{M_l, M_{\underline{J}}} |\langle g|T_q|f\rangle|^2 , \qquad (40)$$

$$R^{xyz}_{p(1/2)J} = \sum_{j,j_1} C_{LSJj\underline{J}} C_{LSJj_1\underline{J}} \langle J_d^{(z)} \cdot l_p^{(x)} \cdot s_p^{(y)} \rangle_f . \qquad (41)$$

We see the same type of expression as in the case $LS \rightarrow J$. This time J is polarized and the effects arise from correlation of the core spin and orbit with this moment.

F. Valence band

In valence-band XPS an electron is ejected from the open shell. This complicates the derivation of formula a bit. For space reasons we will not give them here. The final results are formally the same as for core-hole XPS. For instance, without spin-orbit coupling there are only the $y=0,1$ spectra. The first is the isotropic spectrum; the second measures the total spin of the final state. Likewise, with spin-orbit coupling in the ground state, but neglect of it in the final state, we obtain the $LSJ \rightarrow LS$ result

$$R^{xyz}_{d(1/2)S} = \langle [L_d^{(x)} S_d^{(y)}]^{(z)} \rangle_g \langle [L_d^{(x)} \cdot l_d^{(x)}][S_d^{(y)} \cdot s_d^{(y)}] \rangle_f , \qquad (42)$$

and for $LSJ \rightarrow J$ (lanthanides and actinides), we obtain

$$R^{xyz}_{d(1/2)J} = \langle J_0^{(z)} \rangle_g \langle J_d^{(z)} \cdot l_d^{(x)} \cdot s_d^{(y)} \rangle_f , \qquad (43)$$

which is analogous to the core XPS case. We have omitted the coefficients C appearing in Eqs. (36) and (41) because they contain inessential complicated parentage information. The interpretation here must be in terms of *holes*. L_d, S_d, and J_d are the total moments of the holes in d^n, which are polarized, and l_d and s_d are the moments of the extra hole after photoemission. l_d and s_d are coupled to L_d, S_d, and J_d by Coulomb and spin-orbit interaction, but also by the Pauli principle. For example, when there is only one electron in the ground state, i.e., it is almost completely filled by holes, the extra hole must have its moments antiparallel to the others. In a full shell this effect is absent. Note again that in $\langle\ \rangle_f$ of Eq. (43) the expectation value is taken only on that part of the final state to which the ground state is a parent.

G. Comparison between XPS and x-ray absorption spectroscopy

The Pauli principle gives a few interesting differences between x-ray absorption spectroscopy (XAS) on the one hand and core hole and valence band XPS on the other. In XPS an electron is ejected into a shell which has no interactions. Such a shell is completely isotropic, even if it is considered partly filled, because all levels are degenerate. When a shell does have interactions, at each energy the levels may be polarized, but the integrated intensity is isotropic. Thus the continuum level has no preferences for accepting any specific orientation of the electron and the total intensity is independent of any polarization. This implies that the integrated intensities of all I^{xy} spectra, except I^{00}, are zero.

In XAS the core electron has to find an unoccupied place in the open valence shell. When the valence-shell holes are polarized, the core electron has more possibilities to enter when it has the same polarization. The first consequence of the Pauli principle is that the total intensity of L_3 and L_2 is proportional to the number of holes in the valence shell. The second is that the intensities of both L_3 and L_2 are dependent on the number of vacant $\frac{5}{2}$ and $\frac{3}{2}$ levels, because $p_{3/2}$ and $p_{1/2}$ have different probabilities to change into $d_{5/2}$ or $d_{3/2}$. Because the total spin-orbit interaction of the valence shell is linear in the number of $\frac{5}{2}$ and $\frac{3}{2}$ electrons (or holes), the branching ratio is linear in the spin-orbit energy per hole.[32,33]

The third Pauli effect appears with polarized light, which creates polarized electrons which cannot go freely into a polarized d shell. Therefore, apart from the fine structure, the total intensity and branching ratio are also polarization dependent[34] even in the absence of Coulomb and exchange interactions between core and valence shells. Thus circular dichroism in XAS can be present without core-hole interaction, as has been shown for the transition Cu $d^9 \rightarrow 2p^5 3d^{10}$.[34] The number of independent spectra in XAS is three, for which we can either take the $\Delta J = -1, 0, +1$ spectra or the isotropic, magnetic linear dichroic (MLD) and magnetic circular dichroic (MCD) spectrum.[35]

III. FUNDAMENTAL SPECTRA

In Sec. II we derived that the spin-polarized photoemission process for a given Δl channel is described by eight fundamental spectra I^{xyz}, but only the six $I^{xy} = \sum_z I^{xyz}$ can be measured in practice. Here we will give a simple description of these spectra, which will enable us to understand their nature and the interactions involved. The atomic photoemission process is given pictorially in Fig. 1. It shows a system consisting of a valence state with momenta L_v and S_v and a core state with L_c and S_c, denoting orbital momenta and spin momenta, respectively. In a localized model there are exchange interactions between S_v and S_c and Coulomb and exchange interactions between L_v and L_c, which are indicated in Fig. 1 by dashed lines. The momenta L and S have spin-orbit interaction as indicated by the dotted lines. The valence spin S_v of the ground state has a magnetic polarization m, the electric polarization vector q acts on the core orbital momentum L_c, and the spin polarization σ is measured in S_c. We indicate the polarization by 0, 1, 2, 3 and for isotropic, dipole, quadrupole, and octupole moments, respectively. We may consider x and y to be determined by the experimental setup, i.e., use of polarized light and of a spin-polarization detector with recording of the linear combination of signals defined by I^{xy}. According to Sec. II the magnetic moments needed to measure a $q^x \sigma^y$ spectrum are m^z, where $z = |x-y| \cdots x+y$ ($x+y+z$ is even). For a spectrum to be observable we need interactions connecting the nonzero values of x, y, and z in Fig. 1. The various possibilities I^{xy} are summarized in Table I.

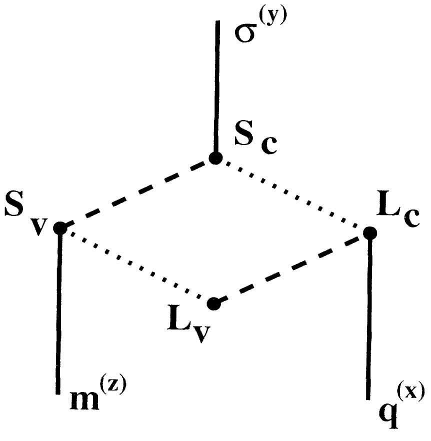

FIG. 1. Schematic picture for spin-polarized photoemission with spin-orbit interactions (dotted lines) and electrostatic interactions (dashed lines). $L_{v(c)}$ and $S_{v(c)}$ denote the orbital and spin momenta of the valence (core) state, respectively; x, y, and z are the polarizations of the electric vector q, spin σ, and magnetic moment m. For a polarization spectrum to be observable, we need interactions connecting the nonzero values of x, y, and z. The various possibilities are summarized in Table I.

A. I^{00}: Isotropic spectrum

The first fundamental spectrum is trivial. This is the isotropic spectrum with no polarizations.

B. I^{01}: Spin spectrum

The electric vector q is isotropic, but m and σ are polarized. It gives the situation with a magnetic dipole moment in the valence band and spin-polarized total emission from the core level excited with isotropic radiation. To couple the m and σ polarization requires at least elec-

TABLE I. Eight fundamental spectra of spin-polarized photoemission in odometer order. $x=0,1,2$ denotes isotropically, circularly, and linearly polarized radiation, respectively. $y=0,1$ denotes without and with spin-polarization measurements, respectively. $z=0,1,2$ denotes a nonisotropic value for $\langle M^z \rangle$, where M is the magnetic moment of the ground state. The columns s.o. and U_{cv} indicate whether spin-orbit and core-valence electrostatic interactions, respectively, are needed to observe I^{xyz}.

Photoemission spectrum	x	y	z	s.o.	U_{cv}
Isotropic spectrum	0	0	0	0	0
Spin spectrum	0	1	1	0	1
Orbit spectrum (MCD)	1	0	1	1	1
Spin-orbit spectrum	1	1	0	1	0
Spin-orbit magnetic quadrupole spectrum	1	1	2	1	1
Anisotropic spectrum (MLD)	2	0	2	1	1
Anisotropic spin magnetic dipole spectrum	2	1	1	1	1
Anisotropic spin magnetic octupole spectrum	2	1	3	1	1

trostatic interaction between S_v and S_c. Thus, from Fig. 1, we can read that with isotropic radiation the total emission from a core level which has electrostatic interaction with the exchange-split valence levels is spin polarized, even in the absence of spin-orbit interaction. The exchange interaction couples the spin of the core and valence holes; neither spin-orbit coupling nor circular polarization is needed.

We have proven in Sec. II that the photoelectron spin polarization depends on the spin in the final state. In the I^{01} spectrum high- (low-) spin final states give positive (negative) peaks (cf. the remark about signs at the end of this section). The intensity of a transition between a pure-spin ground state and a pure-spin final state is the isotropic intensity times a factor

$$I_{SMS'\sigma}=2(2S+1)\left[\begin{matrix} S & \frac{1}{2} & S' \\ -M & \sigma & M' \end{matrix}\right]^2 , \tag{44}$$

where σ is the Z component of the photoelectron spin. The values of the intensities are given in Table II for $M=-S$. The transition to low spin is forbidden for $\sigma=+\frac{1}{2}$ and multiplied by 2 for $\sigma=-\frac{1}{2}$. For the high-spin final state the effect is reversed and smaller by a factor $S/(S+1)$. The relatively simple formula of Eq. (44) still describes I^{10} (but not the other spectra) when the ground state has spin-orbit interaction, as long as it does not mix terms of different spin; in the final-state spin-orbit interactions must be smaller than the experimental resolution.

TABLE II. Factors by which the isotropic intensity of a transition $\sigma=\pm\frac{1}{2}$ has to be multiplied to obtain the intensity in the spin spectrum for a ground-state $S(M=-S)$ to a final-state $S'M'$ in the absence of spin-orbit coupling.

$\Delta S=\pm\frac{1}{2}$	$\sigma=+\frac{1}{2}$	$\sigma=-\frac{1}{2}$
$S'=S+\frac{1}{2}$	$\dfrac{2S+1}{S+1}$	$\dfrac{1}{S+1}$
$S'=S-\frac{1}{2}$	0	2

C. I^{10}: orbit spectrum or magnetic circular dichroism

No spin polarization is measured, but m and q are polarized. MCD requires both spin-orbit and electrostatic interactions (see Fig. 1). In the presence of spin-orbit interaction, the total emission from a core level, which has electrostatic interaction with the exchange-split valence levels, depends on the helicity of the light. The photon spin acts on the orbital momentum of the core electron, which is coupled by electrostatic and spin-orbit interactions to the spin of the valence electrons.

D. I^{11}: spin orbit and spin-orbit magnetic quadrupole spectrum

Both q and σ are polarized; the magnetic polarization must be 0 or 2. It is clear from Fig. 1 that at least core-hole spin-orbit interaction is required, but no interaction with the valence electrons is needed in the $z=0$ contribution. With circularly polarized radiation the total emission from a noninteracting core level with spin-orbit splitting is spin polarized. The photon spin acts on the electron spin via the spin-orbit coupling. In the I^{11} spectrum final states with high (low) core-hole j value give positive (negative) peaks. The spin-orbit spectrum is sometimes called "optical spin orientation." Since no interaction is needed between the core and valence levels, this spectrum can also be obtained in nonmagnetic atoms or in the one-electron model. The value $z=2$ (magnetic quadrupole spectrum) also gives a contribution. In principle, the I^{110} and I^{112} spectra could be measured separately by measuring with, e.g., zero and maximum polarization. The difference is the I^{112} spectrum. We will not treat this further until it comes within reach of experimental possibilities.

E. I^{20}: anisotropic spectrum or magnetic linear dichroism

Since $z=2$ (quadrupole polarization), this effect is present both in ferro- and antiferromagnets, where $\langle M \rangle=0$ but $\langle M^2 \rangle - J(J+1)/3 \neq 0$ when J or $S>\frac{1}{2}$. In the latter case it measures a many-electron effect. A quadrupole can also be induced by a low-symmetry crystal field (keeps M and $-M$ degenerate) together with spin-orbit coupling. The crystal field polarizes at the point L_v in Fig. 1. The effects can be separated by also measuring a magnetically isotropic sample.

The anisotropic spectrum is not spin polarized and depends only on the difference in photoemission with light parallel and perpendicular to the magnetization direction, $(\parallel - \perp)$ which is proportional to Z-polarized minus isotropically polarized emission. The importance of this spectrum is that it is relatively simple to measure.

F. I^{21}: anisotropic spin magnetic dipole and octupole spectrum

The valence band has a magnetic dipole moment, and spin polarization is obtained with linearly polarized light. Spin-orbit as well as Coulomb interactions are needed.

The spectrum represents the spin difference for photoemission with light parallel and perpendicular to the magnetization direction $(\| - \perp)(\uparrow - \downarrow)$. Thus this may be called the anisotropic magnetic spin polarization. In principle, this spectrum contains an I^{211} and I^{213} contribution which can be determined separately with different magnetic polarization, giving information on the magnitudes of both $\langle M \rangle$ and $\langle M^3 \rangle$.

G. Relation between the two Δl channels

The formulation in terms of our fundamental spectra has the advantage that if we know the spectra from core c to one of the continuum states $l = c \pm 1$, we know them also for the other value because they differ only in the factor

$$Q^x_{l1c} = (-1)^{x+l-1-c} \begin{Bmatrix} 1 & 1 & x \\ c & c & l \end{Bmatrix} . \tag{45}$$

Because of the triad $\{c\, c\, x\}$, the values $x = 1$ and 2 are forbidden for s core holes ($c = 0$). From Eq. (45) we can calculate that the lower l_ε channel always has the largest spectra for $x \neq 0$. For $x = 1$ the factors between $c - 1$ and $c + 1$ are always negative, being -2, $-\frac{3}{2}$, and $-\frac{4}{3}$ for c is p, d, and f, respectively. For $x = 2$ they are 10, 3.5, and 2.4, respectively. Our statements about signs of peaks in this section and in Sec. II all refer to the $c - 1$ channel. For $x = 1$ the signs in the $c + 1$ channel are reversed. At high photon energy the $l = c + 1$ channel is strongly dominant and this simple relationship is of little relevance experimentally, except near the Cooper minima. The advantage is mainly in the calculation and analysis of theoretical spectra where we can use the more simple low value of l. Furthermore, the small intensity of the $x = 2$ spectra, because of the factor of 10, means that for both spin polarizations the intensities with Z-polarized and isotropic light are almost the same and $I_{0\uparrow}$ and $I_{0\downarrow}$ do not have to be measured. This means that I^{00}, I^{01}, I^{10}, and I^{11} can be determined approximately in a collinear arrangement with light, sample magnetization, and spin polarization measurement along one axis.

IV. CALCULATIONAL DETAILS

In this section we describe the calculation of the photoemission spectra for Cu, Co, and Fe. The ground state of a divalent Cu ion is a mixture of configurations d^9 and $d^{10}\underline{L}$, where $\underline{L}$ denotes a ligand hole. X-ray photoemission excites a metal c core electron to an l continuum state with no spin-orbit and electrostatic interactions. The corresponding final-state configurations are $\underline{c}d^9 l$ and $\underline{c}d^{10}\underline{L}l$. The configuration interaction in the initial and final states is taken into account using a cluster model.[36,37] The Hamiltonian H_0 can be written as

$$H_0 = H_{\text{ligand}} + H_{\text{metal}} + H_{\text{mix}} + H_{\text{exchange}} + H_{\text{continuum}} , \tag{46}$$

where

$$H_{\text{ligand}} = \sum_{\sigma} E_k l^\dagger_\sigma l_\sigma , \tag{47}$$

$$\begin{aligned} H_{\text{metal}} = {} & \sum_{\nu} E_{d\nu} d^\dagger_\nu d_\nu + \sum_{\nu} E_{c\nu} c^\dagger_\nu c_\nu + \sum_{\nu_1\nu_2\nu_3\nu_4} \langle \nu_1\nu_2 | Q_{cd} | \nu_3\nu_4 \rangle d^\dagger_{\nu_1} d_{\nu_2} c^\dagger_{\nu_3} c_{\nu_4} \\ & + \sum_{\nu_1\nu_2\nu_3\nu_4} \langle \nu_1\nu_2 | U_{dd} | \nu_3\nu_4 \rangle d^\dagger_{\nu_1} d_{\nu_2} d^\dagger_{\nu_3} d_{\nu_4} + \zeta_d \sum_{\nu_1\nu_2} \langle \nu_1 | l\cdot s | \nu_2 \rangle d^\dagger_{\nu_1} d_{\nu_2} + \zeta_c \sum_{\nu_1\nu_2} \langle \nu_1 | l\cdot s | \nu_2 \rangle c^\dagger_{\nu_1} c_{\nu_2} , \end{aligned} \tag{48}$$

$$H_{\text{mix}} = \sum_{\nu} V_\nu (d^\dagger_\nu L_\nu + L^\dagger_\nu d_\nu) , \tag{49}$$

$$H_{\text{exchange}} = -g\mu_B H \sum_{\nu} \langle \nu | S_z | \nu \rangle m_{\sigma\nu} d^\dagger_\nu d_\nu , \tag{50}$$

$$H_{\text{continuum}} = \sum_{\sigma} E_k l^\dagger_\sigma l_\sigma , \tag{51}$$

where $L^\dagger$, $d^\dagger$, $c^\dagger$, and $l^\dagger$ are creation operators for the ligand valence, metal valence, metal core, and continuum holes with energies E_L, E_d , E_c, and E_l, respectively. The index ν labels all orbital and spin quantum numbers. The Hamiltonian H_{ligand} describes the ligand states, which are hybridized with the metal d states as described by H_{mix}, where V is the transfer integral. The Hamiltonian H_{metal} describes the metal states, which are split by spin-orbit interaction $l \cdot s$ with parameters ζ_d and ζ_c, and electrostatic interactions with matrix elements Q_{cd} given by the Slater integrals F^2, G^1, and G^3, and U_{dd} given by the Slater integrals F^2 and F^4.

The Hamiltonian H_{exchange} gives the (super)exchange interaction, which can be treated as a magnetic field acting on the spin only.[38,39] This exchange field lifts the degeneracy, making the energy of the M_J sublevels equal to $-g\mu_B H M_J$, where only the level $M_J = -J$ is populated at $T = 0$ K. It is noted that the exchange splitting cannot be resolved in the final state. Its influence on the spectrum comes from the lifting of the degeneracy in the initial state. $H_{\text{continuum}}$ describes the continuum state with σ labeling its spin and orbital components.

The initial state is given as

$$\begin{aligned} |i_\nu\rangle &= \alpha_\nu |3d^9(\nu)\rangle + \beta_\nu |3d^{10}\underline{L}(\nu)\rangle \\ &= (\alpha_\nu d^\dagger_\nu + \beta_\nu a^\dagger_\nu)|0\rangle , \end{aligned} \tag{52}$$

where $|0\rangle$ is the vacuum state, i.e., the state without valence holes.

The spectra for the ground state of divalent Cu were calculated with an energy separation between the configurations d^9 and $d^{10}\underline{L}$ equal to 1.35 eV.[36,40] The hybridization is given by a transfer integral $V(b_{1g})=2$ eV and

$$V(b_{1g}):V(a_{1g}):V(b_{2g}):V(e_g)=1:\sqrt{1/3}:1/2:1/2\sqrt{2}\ ,$$

for D_{4h} symmetry.[41] This results in a ground state ${}^2B_{1g}$ with 67% d^9 and 33% $d^{10}\underline{L}$ character.

The spectra for the ground state of Co d^7 and Fe d^6 were calculated with spin-orbit coupling and without hybridization.

The transition-matrix elements were calculated using the chain of groups approach exposed by Butler.[42] This approach starts with the calculation of the reduced matrix elements of the necessary operators in the spherical group using Cowan's atomic multiplet program.[43] The Wigner-Eckart theorem is applied to obtain the reduced matrix elements in the desired point group, where the required isoscalar factors are obtained from Butler's point-group program.[42] The values of the parameters for each configuration are given in the figure captions.

The spherical symmetry O_3 is reduced according to $O_3 \supset O_h \supset D_{4h} \supset D_4 \supset C_4$, and its irreducible representations are projected onto representations of the lower group. A magnetic field along the Z axis reduces the symmetry from D_{4h} to C_4 and lifts the Kramer's degeneracy. The exchange field is included by a term $g\mu_B HS$ in the Hamiltonian with $-g\mu_B H=10^{-4}$ eV. The representation for the dipole operator ($J=1$) splits in C_4 symmetry into $q=-1,+1,0$, which corresponds to right and left circularly Z-polarized radiation, respectively.

The core-hold lifetime is taken into account by a convolution of the lines with a Lorentzian.[44]

V. DISCUSSION OF THE CALCULATED SPECTRA

This section discusses the main features of the calculated s and p core-hole and d valence-shell photoemission spectra. These spectra have strongly different features.

A. Core-hole *s* level

For an s level ($c=0$) the only polarization effect is found in the spin spectrum $I^1=I^{01}$. This is necessarily so for $c=0$ because x has to obey the triangular relation $\{ccx\}$ in Eq. (45). I^{11} and I^{21} are zero, which means that left, right, and Z-polarized light make no difference; the orbital of an s state cannot be polarized and it cannot be sensitive to light polarization. In Fig. 1 the connections L_v-L_c and L_c-S_c are absent. This also shows that the only possible polarization effect is the propagation of the ground-state spin polarization to the core-hole spin by core-valence exchange interaction.

According to the analysis in Secs. II and III B for the spin spectrum we may disregard spin-orbit coupling in the ground state when there is no spin-orbit coupling in the final state and we need only to consider spin. For a ground-state spin S the isotropic spectrum consists of two lines with statistical intensity ratio $S+1$: S and an energy splitting equal to the electrostatic interaction $G^1(ns,3d)x(2S+1)/(2l+1)$. Neither the $3d$ spin-orbit nor the d-d interactions influence the spectrum. Figure 2 shows the calculated spectrum for the configuration Fe $d^6({}^5D_4)$. The spin spectrum I^1 consists of two peaks with separation G^1 and, as can be derived from Table II, intensity ratio 1 : -1 for the core-hole spin parallel and antiparallel to the spin of the valence band.

The fact that the spectrum consists of only two lines without multiplet structure is true only when the final-state energy parameters are equal to those in the ground state. In that case the final-state eigenfunctions are given by the ground-state eigenfunctions plus the added core hole with their spins coupled parallel and antiparallel. This is so because Coulomb interactions with an s electron do not mix different valence states.[45] Transitions are only possible to the two states deriving from the ground state.

However, final states with different parentage do mix when the energy parameters in the final state are different from those in the ground state. The Slater integrals F^2 and F^4 with the core hole present are both about 20% larger than without the core hole and give only small changes in our calculation (Fig. 2). But hybridization in the final state should be different from the hybridization in the ground state and could therefore give structure to the spectrum. The Fe $3s$ photoemission has recently been observed by Hillebrecht, Jungblut, and Kisker[15] and Carbone *et al.*[16,17] Their spectra are in accordance with our local model, but the up-spin peak is much broader than the down-spin peak. A possible explanation would be that the up-spin states have a stronger hybridization with the exchange-split band states. If this explanation is correct, the s core-hole spin spectrum is an ideal tool to study hybridization effects because other effects are absent. Of course, a localized model is not the best way to describe these final-state effects in a metal.[46]

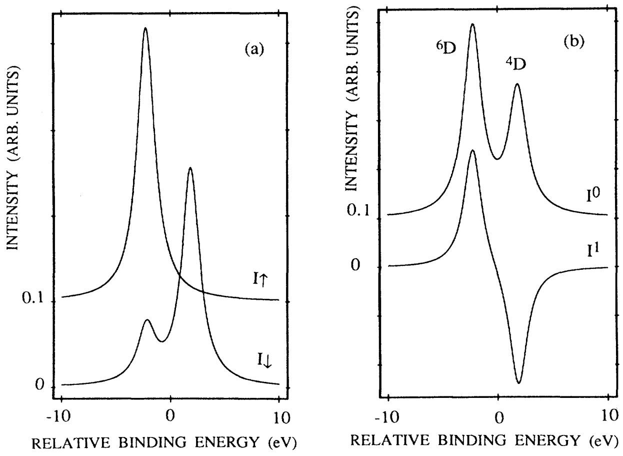

FIG. 2. Fe core s spin-polarized photoemission: (a) the ↑ and ↓ spectrum and (b) the isotropic spectrum I^0 and spin spectrum I^1 for the transition Fe $3d^6({}^5D_4)\rightarrow ns^2 3d^6 \epsilon p$. The Slater integral $G^1(ns,3d)$ is 4.1 eV. Broadened with a Lorentzian of $\Gamma=1$ eV.

B. Noninteracting p level

Before discussing the emission of an interacting level, we will first look at a noninteracting p level as realized in, e.g., a d^0 or d^{10} ground state. In this case there is only an I^{11} spectrum, where the polarization of the photoelectron is caused by the spin-orbit coupling of the core hole. The spectrum consists of two lines ($j=\frac{3}{2}$ and $\frac{1}{2}$) and is therefore completely determined by the branching ratio, since the total intensity is constant. Table III gives the branching ratio both for $p \rightarrow s_\varepsilon$ and $p \rightarrow d_\varepsilon$ transitions of all primitive spectra: $1\uparrow$ $(=-1\downarrow)$, $0\uparrow$ $(=0\downarrow)$, and $-1\uparrow$ $(=1\downarrow)$ with dipole component $(-1,0,1)$ and spin $(\uparrow,\downarrow)$. Linear polarization gives a statistical ratio. For $p \rightarrow s_\varepsilon$ the $p_{1/2}$ transition is forbidden with right circular light ($\Delta m=+1$), which makes its branching ratio equal to 1. For transitions $p \rightarrow d_\varepsilon$ the effect is reversed and half as large. This large anisotropy in the spin polarization will appear in any XPS from a deep core hole with large spin-orbit coupling. Coulomb interactions between p and d cause deviations from these branching ratios, but the order of magnitude is correct.

C. Core-hole $2p$ level

Figures 3, 4, and 5 show the $2p$ XPS of Cu d^9, Co d^7, and Fe d^6, respectively. Although the Cu calculations are in D_{4h}, we will see that most of our spherical analysis is still valid. We show the fundamental spectra for the $\Delta l=-1$ channel because the effects are larger in this channel, providing a natural scaling factor. Also, for this channel the sign of the peaks is as described in Sec. II. For the $\Delta l=+1$ channel the spectra with $x=1$ must be divided by -2 and those with $x=2$ by 10.

The I^{01} spectrum shows the spin of the final states. In Cu with a ground state $^2b_1$ the large $p^5d^{10}\underline{L}$ peaks show a small signal because in this configuration there are no Coulomb interactions separating triplet and singlet peaks. The satellites do have Coulomb interactions, and we see on each satellite a positive low-energy side (triplet) and a negative high-energy side (singlet) according to Hund's rule. Here the mutual alignment of core-hole spin and polarized valence-band spin is parallel and antiparallel, respectively. In the I^{10} spectrum we see the alignment of the core l vector with respect to the polarized valence electron. Because of the core spin-orbit interaction, l is parallel to the core spin in $p_{3/2}$ and antiparallel in $p_{1/2}$. Therefore, I^{10} and I^{01} are very similar, only changing the relative sign between $p_{3/2}$ and $p_{1/2}$. This is a feature common to all deep core holes. In ferromagnetic Fe Baumgarten *et al.*[2] observed an I^{10} Fe $2p$ spectrum which shows an antisymmetric shape for both edges, but with opposite signs. This structure has been discussed elsewhere.[19]

In Co and Fe we see more clearly than in Cu the importance of the spin spectrum when there is Coulomb interaction in the final state. The $p_{3/2}$ peak generally starts with a large high-spin peak followed by a smaller low-

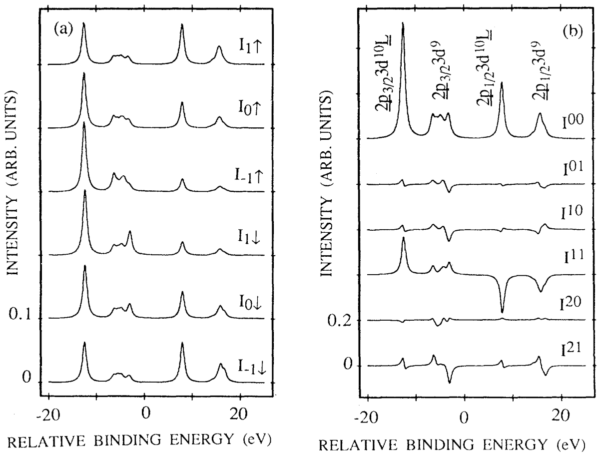

FIG. 3. Cu $2p$ spin-polarized photoemission: (a) primitive spectra and (b) fundamental spectra (see Table I) for the transition Cu $\alpha 3d^9+\beta 3d^{10}\underline{L} \rightarrow \alpha' 2p^5 3d^9 \varepsilon d+\beta' 2p^5 3d^{10}\underline{L}\varepsilon d$. For $3d^9$, $\zeta_{3d}=0.13$, $\Delta=1.35$, and $Q=7.95$ eV; see Sec. IV for further details of the ground state. The $2p^5 3d^9$ configuration has $\zeta_{2p}=13.60$, $\zeta_{3d}=0.13$ eV, and Coulomb interactions $Q_{2p,3d}$ given by $F^2=7.74$, $G^1=5.62$, and $G^3=3.21$ eV. Broadened with a Lorentzian of $\Gamma=0.5$ eV. The given fundamental spectra are as defined by Eqs. (9)–(14), but without the constant factors.

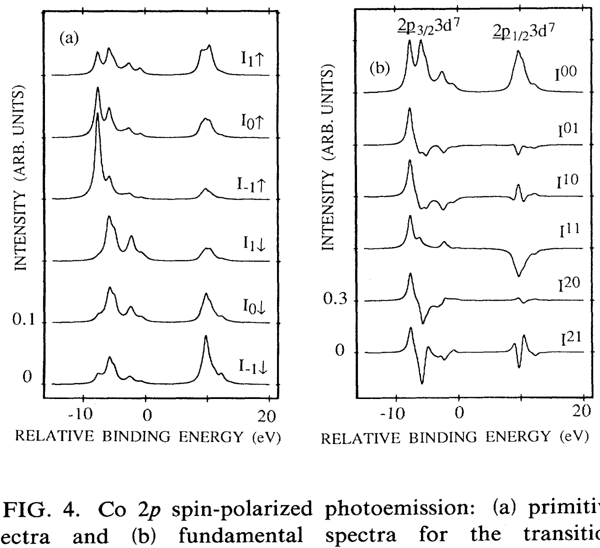

FIG. 4. Co $2p$ spin-polarized photoemission: (a) primitive spectra and (b) fundamental spectra for the transition Co $3d^7(^4D_{9/2}) \rightarrow 2p^5 3d^7 \varepsilon d$. Co$3d^6$: $F^2=9.28$, $F^4=5.77$, and $\zeta_{3d}=0.066$ eV. Co $2p^5 3d^6$: $F^2(dd)=10.74$, $F^4(dd)=6.71$, $\zeta_{3d}=0.092$, $\zeta_{2p}=9.75$, $F^2(pd)=6.32$, $G^1(pd)=4.76$, and $G^3(pd)=2.71$ eV. Broadened with a Lorentzian of $\Gamma=0.5$ eV.

TABLE III. Branching ratio $p_{3/2}/(p_{1/2}+p_{3/2})$ in the $I_{q\sigma}$ spectra for the transition $p^6(^1S) \rightarrow p_j^5 \varepsilon l$, with $l=s,d$, dipole component $q=-1,0,+1$, and spin $\sigma=\uparrow,\downarrow$.

$I_{q\sigma}$	Branching ratio $p_j^5 \varepsilon s$	Branching ratio $p_j^5 \varepsilon d$
$I_{1\uparrow}$ $(=I_{-1\downarrow})$	1	1/2
$I_{0\uparrow}$ $(=I_{0\downarrow})$	2/3	2/3
$I_{-1\uparrow}$ $(=I_{1\downarrow})$	1/3	5/6

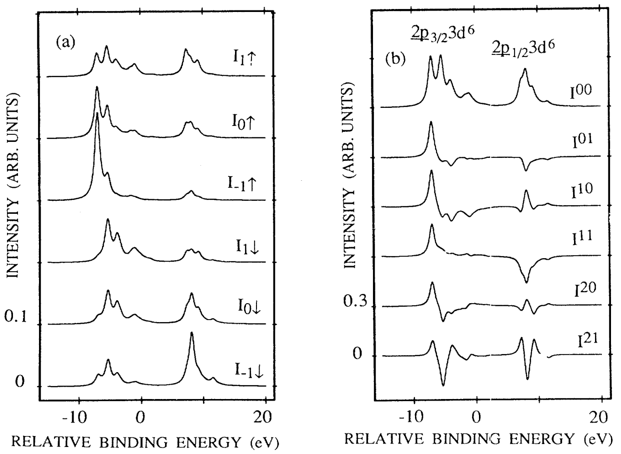

FIG. 5. Fe 2*p* spin-polarized photoemission: (a) primitive spectra and (b) fundamental spectra for the transition Fe $3d^6(^5D_4)\to 2p^53d^6\varepsilon d$. Fe $3d^6$: $F^2=8.77$, $F^4=5.45$, and $\zeta_{3d}=0.052$ eV. Fe $2p^53d^6$: $F^2(dd)=10.25$, $F^4(dd)=6.42$, $\zeta_{3d}=0.074$, $\zeta_{2p}=8.20$, $F^2(pd)=5.94$, $G^1(pd)=4.44$, and $G^3(pd)=2.52$ eV. Broadened with a Lorentzian of $\Gamma=0.5$ eV.

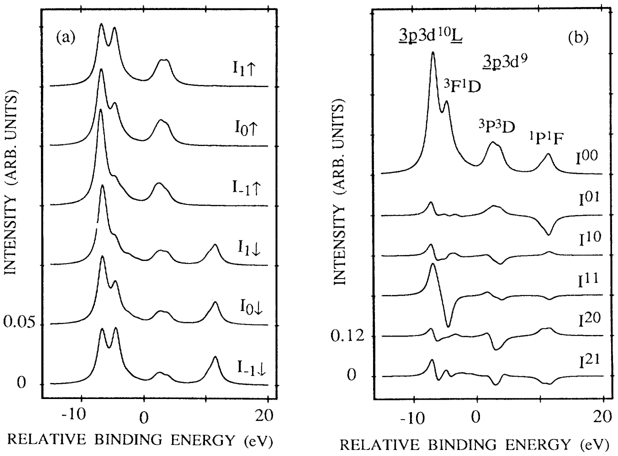

FIG. 6. Cu 3*p* spin-polarized photoemission: (a) primitive and (b) fundamental spectra for the transition Cu $\alpha 3d^9+\beta 3d^{10}\underline{L}\to\alpha' 3p^53d^9\varepsilon d+\beta' 3p^53d^{10}\underline{L}\varepsilon d$. Cu $3d^9$: $\zeta_{3d}=0.13$ eV. Cu $3p^53d^9$: $\zeta_{3p}=1.50$, $\zeta_{3d}=0.13$ eV, $F^2=14.6$, $G^1=18.0$, and $G^3=11.0$ eV. Broadened with a Lorentzian of $\Gamma=0.8$ eV.

spin part. In the $p_{1/2}$ peak there is only a low-spin peak. The absence of a positive peak in $p_{1/2}$ is not understood. Apparently, the high- and low-spin regions overlap completely with low spin always in the majority. The spin-orbit spectrum I^{11} invariably shows a positive $p_{3/2}$ and a negative $p_{1/2}$ peak, as expected. However, in Co and Fe the second main peak of $p_{3/2}$ is strongly suppressed as compared to the first. Of course, $j=\frac{3}{2}$ is not an exact quantum number, but apparently the consequences of this are concentrated in the second peak. The spectra I^{20} and I^{21} are much weaker (in the $p\to d$ channel) than the others and are more difficult to interpret. A free-atom configuration Cu $d^9(^2D)$ has no I^{20} spectrum because $S=\frac{1}{2}$ only gives $z=0$ and 1; the weak structure in Fig. 3(b) is induced by the anisotropic hybridization.

D. Core-hole 3*p* level

The Cu 3*p* spectra are shown in Fig. 6 in the same manner as described in Sec. V C. The $\underline{3p}3d^9$ spectrum is split by *p*-*d* Coulomb interactions, and near its low-energy side there is the $\underline{3p}3d^{10}\underline{L}$ configuration.[36] The spin assignment is immediately clear in the spin spectrum I^{01}, which clearly shows the $^1P,^1F$ and $^3P,^3D$ peaks. The $d^{10}\underline{L}$ peak gives a structure with high spin at the low-energy side.

The spin-orbit spectrum I^{11} shows that $^1P,F$ and $^3P,D$ have only small spin-orbit interactions. The strongest effect is seen in the low-energy structure. $p^5d^{10}\underline{L}$ has no Coulomb interactions of itself; spin-orbit coupling can show its full effect. By the mixing with $^3F,^1D$, this effect is spread over the whole low-energy structure. The 3*p* spin spectrum of Fe metal has been measured already.[18] It has no apparent multiplet structure. The present incompleteness of the theory of core-hole interactions in metallic systems precludes a discussion of the relevance of this spectrum to localized systems.

The orbit spectrum I^{10} shows that l_p is aligned antiparallel to the *d* spin in the $^3P,D$ and $^1P,F$ peaks and parallel at the low-energy side. This may be explained as follows: L_d is aligned with S_d. In *F* states, l_p is aligned with L_d and thus with S_d [Eq. (36)]. In *D* states, l_p and L_d are not aligned and in *P* states they are antiparallel. In the $\underline{pd}^{10}\underline{L}$ peak L_d is not aligned.

E. Valence band

In Fig. 7(b) we show the Cu valence-band photoemission spectrum.[36,40] As in the 3*p* spectrum, the spin spec-

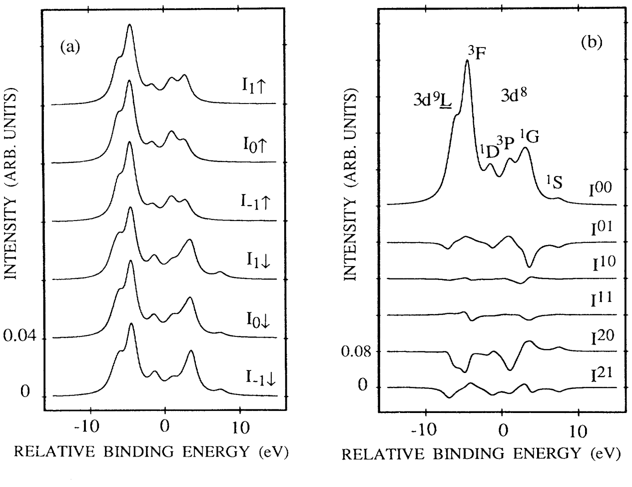

FIG. 7. Cu valence-band spin-polarized photoemission: (a) primitive spectra and (b) fundamental spectra for the transition Cu $\alpha 3d^9+\beta 3d^{10}\underline{L}\to\alpha' 3d^8\varepsilon f+\beta' 3d^{10}\underline{L}\varepsilon f$. Cu $3d^9$: $\zeta_{3d}=0.13$ eV. Cu $3d^8$: $F^2=11.11$, $F^4=6.94$, and $\zeta_{3d}=0.13$ eV. Broadened with a Lorentzian of $\Gamma=0.8$ eV.

trum I^{01} gives very direct and clear information on the final-state spin. The other spectra need detailed analysis to determine the origin of their structure. The I^{20} spectrum must originate from the hybridization (making the symmetry D_{4h}) because the $S=\frac{1}{2}$ ground state cannot have $z=2$. Also, part of the I^{11} spectrum probably comes from a $z=2$ contribution. This also holds for the Cu $2p$ and $3p$ spectra, of course. In the valence-band photoemission the I^{20} spectrum is relatively strong; in the figure we show the fundamental spectra for $d \rightarrow p_\varepsilon$, but the $d \rightarrow f_\varepsilon$ spectra for $x=2$ are only a factor 3.5 less intense (cf. Sec. III).

VI. CONCLUSIONS

Measurement of the spin polarization in photoemission of localized magnetic systems greatly increases the amount of information on the magnetic moment of the ground state and on the interaction of this moment with the spin and orbit of the hole created. This is equally valid for deep and shallow core-hole XPS and valence-band XPS. In this paper we show some spectra of Cu, Co, and Fe and give an analysis which also applies to rare-earth ions and to the experimentally observed spin polarization in Fe $3s$ XPS and the magnetic circular dichroism in Fe $2p$ XPS.

The analysis of the spectra acquires great precision by a unified description which includes all polarized XPS techniques with and without circularly or linearly polarized light, spin-polarization detection, and magnetic polarization of the sample, but excluding emission-angle-dependent measurement. Suitable sum and difference spectra produce eight *fundamental* spectra which contain very specific information. Although, by varying the polarization of the incident light and detected spin only six spectra of these eight can be separated, the full set can be obtained by preparing different magnetic ground states.

The unified analysis has the following features.

(i) It systematizes all polarized XPS techniques, provides an overview over the complex of possibilities, and makes it easier to choose the right method for the problem at hand, given the technical possibilities.

(ii) It shows why the spectrum with light polarization parallel to the magnetic moment is almost equal to the isotropic spectrum for $p \rightarrow d_\varepsilon$ transitions. This makes it possible to obtain the most important fundamental spectra in a collinear experimental arrangement with the light, magnetic moment, and spin-polarization measurement along one axis.

(iii) It shows that the $\Delta l = -1$ spectra can be obtained in a simple way from the $\Delta l = +1$ spectra. The spectra contain exactly the same information. This also implies that theoretical analysis is simplified because we only have to do the more simple $\Delta l = -1$ calculations.

(iv) It derives what information is contained in each fundamental spectrum about the interaction between the polarized valence shell and the hole created.

The analysis further shows that in order to measure all effects both circularly and linearly polarized radiation is required (see Table I). With linear polarization one cannot measure magnetic circular dichroism and spin-orbit effects, whereas with circular polarization one cannot measure the anisotropies. Only the "spin spectrum" uses isotropic light. Without spin detection information about the magnetic ground state can be obtained from magnetic dichroism. Again, circular and linear polarization are complementary. The former gives the expectation value of the magnetic moment; the latter gives the *absolute value* of the magnetic moment, allowing one to measure antiferromagnetic materials.

Spin-polarized core-hole photoemission is complementary to other magnetic techniques. Unlike magneto-optical effects in optical spectroscopy, it probes the magnetic moment of only those electrons which have electrostatic interaction with the core hole; and contrary to neutron diffraction, paramagnetic resonance, susceptibility measurements, and Mössbauer spectroscopy, it provides information about the *local* magnetic structure. The well-defined wave function of the core hole offers an approach different from optical spectroscopy, because it gives element and site selectivity. The spectra can be analyzed using an atomic calculation including crystal field, hybridization (mixing), and configuration interaction. The analysis can be applied generally to transition-metal, rare-earth, and actinide compounds with localized valence electrons with their large variety of magnetic structures. Compared to magnetic x-ray dichroism, the added information from the spin polarization allows a deeper analysis.

---

[1] U. Fano, Phys. Rev. **178**, 131 (1969).

[2] L. Baumgarten, C. M. Schneider, H. Petersen, F. Schäfers, and J. Kirschner, Phys. Rev. Lett. **65**, 492 (1990).

[3] L. C. Davis, J. Appl. Phys. **59**, 25 (1986).

[4] J. Kanamori and A. Kotani, *Core-Level Spectroscopy in Condensed Systems*, Vol. 81 of *Springer Series in Solid-State Sciences* (Springer-Verlag, Heidelberg, 1988).

[5] E. Beaurepaire, B. Carriere, and J. P. Kappler, *Rayonnement Synchrotron Polarisé, Electrons Polarisés et Magnétisme* (L'imprimé, Strasbourg, 1990).

[6] J. B. Goedkoop, J. C. Fuggle, B. T. Thole, G. van der Laan, and G. A. Sawatzky, Nucl. Instrum. Methods Phys. Res. A **273**, 429 (1988).

[7] A. H. Forman, Phys. Rev. **3**, 306 (1914); **7**, 119 (1916).

[8] G. van der Laan, B. T. Thole, G. A. Sawatzky, J. B. Goedkoop, J. C. Fuggle, J. M. Esteva, R. Karnatak, J. P. Remeika, and H. A. Dabkowska, Phys. Rev. B **34**, 6529 (1986).

[9] D. Gibbs, D. R. Harshman, E. D. Isaacs, D. B. McWhan, D. Mills, and C. Vettier, Phys. Rev. Lett. **61**, 1241 (1988).

[10] J. P. Hannon, G. T. Trammell, M. Blume, and D. Gibbs, Phys. Rev. Lett. **61**, 1245 (1988).

[11] E. D. Isaacs, D. B. McWhan, C. Peters, G. E. Ice, D. P. Siddons, J.B. Hastings, C. Vettier, and O. Vogt, Phys. Rev. Lett. **62**, 1671 (1989).

[12] C. Kao, J.B. Hastings, E. D. Johnson, D. P. Siddons, G. C. Smith, and G. A. Prinz, Phys. Rev. Lett. **65**, 373 (1990).

[13] J. Bonarski and J. Karp, J. Phys. Condens. Matter **1**, 9261 (1989).

[14] D. P. Siddons, M. Hart, Y. Amemiya, and J. B. Hastings, Phys. Rev. Lett. **64**, 1967 (1990).

[15] F.U. Hillebrecht, R. Jungblut, and E. Kisker, Phys. Rev. Lett. **65**, 2450 (1990).

[16] C. Carbone, T. Kachel, R. Rochow, and W. Gudat, Z. Phys. B **79**, 325 (1990).

[17] C. Carbone, T. Kachel, R. Rochow, and W. Gudat, Solid State Commun. **77**, 619 (1991).

[18] C. Carbone and E. Kisker, Solid State Commun. **65**, 1107 (1988).

[19] G. van der Laan, Phys. Rev. Lett. **66**, 2527 (1991).

[20] G. van der Laan, J. Phys. Condens. Matter **3**, 1015 (1991).

[21] F. Meier and B. P. Zakharchenya, *Optical Orientation* (North-Holland, Amsterdam, 1984).

[22] R. Feder, *Polarized Electrons in Surface Physics* (World Scientific, Singapore, 1985).

[23] J. Kischner, *Polarized Electrons at Surfaces* (Springer-Verlag, Heidelberg, 1985).

[24] U. Bänninger, G. Busch, M. Campagna, and H. C. Siegmann, Phys. Rev. Lett. **25**, 585 (1970).

[25] N. A. Cherepkov, Zh. Eksp. Teor. Fiz **65**, 933 (1973) [Sov. Phys.—JETP **38**, 463 (1974)].

[26] C. M. Lee, Phys. Rev. A **10**, 1598 (1974).

[27] G. Schönhense, Phys. Scr. T **31**, 255 (1990).

[28] Cherepkov and Kuznetsov, J. Phys. B **22**, L405 (1989).

[29] R. L. Dubs, S. N. Dixit, and V. McKoy, Phys. Rev. Lett. **54**, 1249 (1985).

[30] D. M. Brink and G. R. Satchler, *Angular Momentum* (Oxford University Press, London, 1962).

[31] A.P. Yutsis, I. B. Levinson, and V. V. Vanagas, *Mathematical Apparatus of the Theory of Angular Momentum* (Israel Program for Scientific Translation, Jerusalem, 1962).

[32] B. T. Thole and G. van der Laan, Phys. Rev. A **38**, 1943 (1988).

[33] B. T. Thole and G. van der Laan, Phys. Rev. B **38**, 3158 (1988).

[34] G. van der Laan and B. T. Thole, Phys. Rev. B **42**, 6670 (1990).

[35] B. T. Thole, G. van der Laan, and G. A. Sawatzky, Phys. Rev. Lett. **55**, 2086 (1985).

[36] G. van der Laan, C. Westra, C. Haas, and G. A. Sawatzky, Phys. Rev. B **23**, 4369 (1981).

[37] K. Okada and A. Kotani, J. Phys. Soc. Jpn. **58**, 2578 (1989); J. Electron Spectrosc. Relat. Phenom. **52**, 313 (1990).

[38] J. B. Goodenough, Phys. Chem. Solids **6**, 287 (1958).

[39] J. Kanamori, Phys. Chem. Solids **10**, 87 (1959).

[40] A. Kotani, K. Okada, S. Tanaka, and Y. Seino, in *Strong Correlation and Superconductivity*, edited by H. Fukuyama, S. Maekawa, and A. P. Malozemoff, Vol. 89 of Springer Series in Solid-State Sciences (Springer-Verlag Berlin, Heidelberg, 1989), p. 77.

[41] H. Eskes, L. H. Tjeng and G. A. Sawatzky, Phys. Rev. B **41**, 288 (1990).

[42] P. H. Butler, *Point Group Symmetry, Applications, Methods and Tables* (Plenum, New York, 1981).

[43] R. D. Cowan, *The Theory of Atomic Structure and Spectra* (University of California Press, Berkeley, 1981).

[44] J.C. Fuggle and S.F. Alvarado, Phys.Rev. A **22**, 1615 (1980).

[45] Equations 12.70–12.72 in Ref. 43.

[46] Y. Kakehashi, K. Becker, and P. Fulde, Phys. Rev. B **29**, 16 (1984).